ORIGINAL ARTICLE

UDC: 616.8:616-006
https://doi.org/10.2298/VSP161215103M

The application of the local histograms of apparent difusion coefficient in differentiation of brain astrocytomas

Primena lokalnih histograma prividnog difuzionog koeficijenta u diferencijaciji astrocitoma mozga

Jelena Mihailović*, Danica Grujičić*†, Slobodan Lavrnić‡, Marko Daković†§

***National Cancer Research Center, Belgrade, Serbia; Clinical Center of Serbia, †Clinic for Neurosurgery, ‡Center for Radiology and Magnetic Resonance, Belgrade, Serbia; University of Belgrade, §Faculty of Physical Chemistry, Belgrade, Serbia**

Abstract

Background/Aim. Microstructural diversity of brain astrocytomas makes their diagnostics and differentiation by using the diffusion weighted imaging (DWI) difficult. In this study we used the histogram-based positioning of regions of interests on the apparent diffusion coefficient (ADC) maps in order to restrict the determination of diffusion parameters to regions of interest (ROI) corresponding to maximum cellularity. Success of ADC standard deviation (ΔADC) and kurtosis (K) in differentiation of brain astrocytomas was evaluated. **Methods.** The thirtyone patients (16 women and 15 men, median age 37 years, age range 6–72 years) with suspected supratentorial astrocytomas were included in the retrospective study. The magnetic resonance imaging (MRI) examinations were performed using the 1.5 T MR system (Avanto; Siemens, Erlangen, Germany) and 8-channel phased array head coil. The DWI images were acquired in three orthogonal directions for the b-values 0, 500 and 1000 s mm^{-2}. The histogram calculations and determination of diffusion parameters were performed using the MIPAV software package and the statistical analysis was done in the Openstat software. **Results.** The ADC values enabled differentiation of diffuse astrocytomas (DA) from a high-grade astrocytoma (HGA), but not between the classes of HGA. In addition, the ΔADC value provided discrimination between the anaplastic astrocytoma (AA) and glioblastoma multiforme (GBM) with 100% of sensitivity and 89% of specificity . The kurtosis value can also differentiate between the grades AA and GBM although with the lower sensitivity and specificity. **Conclusion.** The histogram analysis of tumor region on the ADC maps can provide a guidance for an appropriate choice of the ROIs. The parameters which characterize diffusion of such defined ROIs, as well as their combination can improve differentiation of brain astrocytomas.

Key words:
astrocytoma; neoplasm staging; histology; diffusion magnetic resonance imaging.

Apstrakt

Uvod/Cilj. Razlikovanje atrocitoma mozga zasnovano na analizi mapa difuzijski naglašenog snimanja (DWI) predstavlja težak zadatak, što je posledica mikrostrukturne heterogenosti ovih entiteta. U ovoj studiji primenjena je histogramska analiza mapa prividnog difuzionog koeficijenta (ADC) da bi se lokalizovali regioni (ROI) koji odgovaraju maksimalnoj celularnosti tumora. Testirana je mogućnost korišćenja parametara dobijenih iz tih regiona [ADC, standardna devijacija ADC (ΔADC) i kurtozis (K)] za razkovanje različitih gradusa astrocitoma. **Metode.** U retrospektivnu studiju bio je uključen 31 bolesnik (16 žena i 15 muškaraca, prosečna starost 37 godina; raspon 6–72 godina) sa suspektnim supratentorijalnim astrocitomima. Pregledi magnetno rezoanantnim snimanjem (MRI) urađeni su na uređaju jačine magnetnog polja 1,5 T (Avanto; Siemens, Erlangen, Nemačka). Korišćena je 8-kanalna zavojnica za glavu. DWI snimci dobijeni su u tri međusobno normalna pravca i tri vrednosti difuzijske ostetljivosti b (0, 500 and 1000 s mm^{-2}). Histogramska analiza i određivanje difizionih parametara izvršeno je korišćenjem MIPAV sofvera. Statistička analiza urađena je u Openstat programskom paketu. **Rezultati.** Ustanovljena je statistički značajna razlika između ADC vrednosti za difuzne astrocitome (DA) i visokogradusne astrocitome (HGA), ali ne i između HGA podklasa. Statistički značajne razlike nađene su i između ΔADC vrednosti za anaplastične astrocitome (AA) i glioblastome mulitforme (GBM) za 100% osetljivošću i 89% specifičnosti. K parametar takođe može poslužiti u razlikovanju AA i GBM ali sa manjom osetljivošću i specifičnošću. **Zaključak**. Histogramska analiza regiona tumora na ADC mapama može po-

Correspondence to: Marko Daković, University of Belgrade, Faculty of Physical Chemistry, Studentski trg 12, 11 000 Belgrade, Serbia. E-mail: marko@ffh.bg.ac.rs

služiti kao vodič za pravilno pozicioniranje ROI. Parametri koji karakterišu difuziju na tako definisanim ROI, pojedinačno i kombinovano, mogu pomoći u diferencijaciji astrocitoma mozga.

Ključne reči:
astrocitom; neoplazme, odredjivanje stadijuma; histologija; magnetna rezonanca, difuziona.

Introduction

Astrocytic tumors are the most frequent brain neoplasmas which comprise about two- thirds of brain gliomas. The choice of appropriate therapeutic strategy largely relies on the assessment of histopatological grade of tumor. Stereotactic biopsy is an option, but the pronounced structural heterogeneity of astrocytomas, which even may manifest in coexistence of two distinct histological types within tumor bulk [1], can lead to sampling errors. The method for the non-invasive assessment of grade and localization of the most active segments of tumors would significantly improve diagnostics and treatment of these tumors.

The conventional magnetic resonance imaging (MRI) presents the backbone of the brain tumor imaging. Although the techniques of T1 weighted (T1W), T2 weighted (T2W), the fluid attenuated inversion recovery (FLAIR) and gadolinium enhanced T1W imaging provide a good qualitative interpretation, they lack in specificity in tumor grading [2]. It has been generally agreed that the dynamic contrast enhanced (DCE) imaging tracing regions of increased capillarity and neovascularization can distinguish between the low and high grade gliomas, but not within the groups (although there are some different opinions [3, 4]). This could be attributed to the fact that the differences in cellularity may not always coincide with the differences in capillarity.

Diffusion weighted imaging (DWI) is an advanced MRI technique which provides unique information about microstructure of tissues by probing self-diffusion of water molecules. Microscopic movements of water molecules are mostly affected by the presence of cell membranes, which, due to low permeability for water as compared to the free diffusion, represent a barrier for unhindered movement of water molecules [5–7]. Therefore, any alteration in cell density or size will affect water diffusion in tissue and the extent of hindrance can be quantified by the apparent diffusion coefficient (ADC) as measured on the DWI.

The differentiation of brain astrocytomas (BA) using the DWI represents challenge from a viewpoint of the DWI because of their microstructural diversity. Despite the well-established correlation between the ADC values and tumor cellularity [8–12], this, apparently straightforward approach, produced a variety of results. Some authors found that the ADCs could not be used to separate different tumor grades [13–15] while others managed to differentiate a low- from a high-grade tumors, but not between the subtypes [8, 9, 16–20]. The discrepancies in results of these studies can be explained by two inter-related factors: a placement of the region of interest (ROI) for the ADC measurement and structural peculiarities of astrocytoma. Namely, the results were obtained by placing the ROI on a selected representative section of the tumor based on their appearance on the selected images. Such approach relies on *a priori* knowledge about the tumor structure introducing subjectivity and effects of sampling in analysis. To overcome that problem, some authors [21, 22] opted to place the ROI over the entire tumor and analyze obtained histograms of ADC values within the tumor. By using this approach, a successful differentiation was achieved within the group of a low grade as well as between a low- and a high-grade astrocytoma (HGA).

Diffusion MR imaging offers other potentially useful techniques, besides measurements of the ADC, in characterization of the brain lesions which were attempted in grading of BA. The diffusion tensor imaging (DTI) depicts the degree of directionality of water molecules movements. The fractional anisotropy (FA) maps of water diffusion confirmed that these pathologies in general show the lower FA values compared to normal white matter, because of displacement and/or destruction of axonal tracts [23–25]. However, only a coarse separation of the low- from high-grade tumors has been achieved [15, 26]. Recently introduced technique, the diffusion kurtosis imaging (DKI) evaluates structurallity of tissue by quantifying of departure of water molecules displacements from the Gaussian distribution. The measure of this is dimensionless parameter named excessive diffusion kurtosis (EDK) [27, 28]. In general, the technique showed the remarkable success in neural tissue characterization [27, 29]. The initial results in the differentiation of BA grades based on the mean EDK are promising [30].

In this paper, we used both advanced strategies in better differentiation of brain astrocytomas: analysis of the texture of tumor on the ADC maps by histograms as the guidance for placing the ROIs in the areas of the minimal ADCs; beside using just the ADCs, we determined parameters which describe microheterogeneity within the selected ROIs – standard deviation of ADC (ΔADC) and kurtosis (K) to evaluate the added values of the DWI. The principal aim of this study was differentiation between subtypes of HGA.

Methods

Patients

Thirty-one patients (16 women and 15 men, median age 37 years, age range 6–72 years) with the suspected supratentorial glial tumors were included in this retrospective study. The study was approved by the Ethics boards of our institutions. Informed consent was obtained from all examined patients. The subjects with the recurrent gliomas were excluded from the evaluation. After the MRI examination, all patients underwent surgery and the histological diagnosis was provided by the analysis of post-operative specimens. The analysis revealed the presence of 13

diffuse astrocytoma [World Health Organization (WHO) grade II], 9 anaplastic astrocytoma (AA) (WHO grade III), and 9 glioblastoma multiforme (GBM, WHO grade IV).

Magnetic resonance imaging methods

The MRI examinations were performed using the 1.5 T MR system (Avanto; Siemens, Erlangen, Germany) and 8-channel phased array head coil. Conventional MR images were obtained using the T_1 weighted [spinecho (SE), TR = 550, TE = 10 ms] and turbo T_2 weighted [turbo spin echo (TSE), 4800/94], both with 5 mm slice thickness and 1 average. The DWIs were acquired using a single-shot echo-planar imaging sequence (TR = 3800, TE = 89 ms); twenty-five sections of 5 mm thickness were obtained (field of view 230 × 230, matrix size 191 × 192) in three orthogonal direction for b-values 0, 500 and 1000 $s \cdot mm^{-2}$. In cases where the presence of blood/blood derivates were suspected, the gradient echo (T2*) sequence (TR = 847, TE = 25 ms and flip angle 20°) was conducted. This was observed in one case of anaplastic astrocytoma (11%) and in four cases of GBM (45%).

Afterwards, the paramagnetic contrast agent (0.1 $mmol \cdot kg^{-1}$) was administered and the T_1W sagital sections were acquired using the magnetization prepared rapid acquisition gradient echo (MPRAGE) sequence (TR/TE = 2000/4.7, slice thickness 0.9 mm). The post-contrast coronal and axial 5 mm thick sections were obtained from these images using a reconstruction algorithm included in the software of MRI workstation.

Determination of parameters on apparent diffusion coeficient images

Upon the completion of the MR exam, all data were exported to the personal computer workstation with the Ubuntu 14.04 operating system. The MIPAV software (National Institute of Health, Bethesda, USA) [31] was used for determination of the ADC, ΔADC, and K on the ROI. In the first step, the T2W images were matched with the size and resolution of the DWI/ADC images ("Match images" alghoritm in the Mipav). The regions of hyperintensity on three consecutive T_2W slices (the middle one matching to maximal tumor diameter) were manually delineated (primary ROIs) and transferred by copying to the corresponding ADC maps. The areas that coincide to the presence of blood/blood products as seen on the T_2^*W images were excluded. Second, a histogram of ADC was obtained and histogram-based color maps were generated for the primary ROI (Figure 1C). The total of six ROIs of equal size (12 pixels) were placed in the areas which coincide with the blue regions (hypointensities) on those maps (Figure 1, right). The values of parameters (ADC, ΔADC, K) were determined by averaging those from individual ROIs. The histogram analysis of corresponding color coding of tumor was presented in Figure 1B. The kurtosis parameter, which defines the "peakedness" of distribution of measured values, were closely connected to the standard deviation by the equation $K = \frac{\mu_4}{\sigma^4}$ (1) where μ_4 is the fourth moment about the mean and σ is the standard deviation.

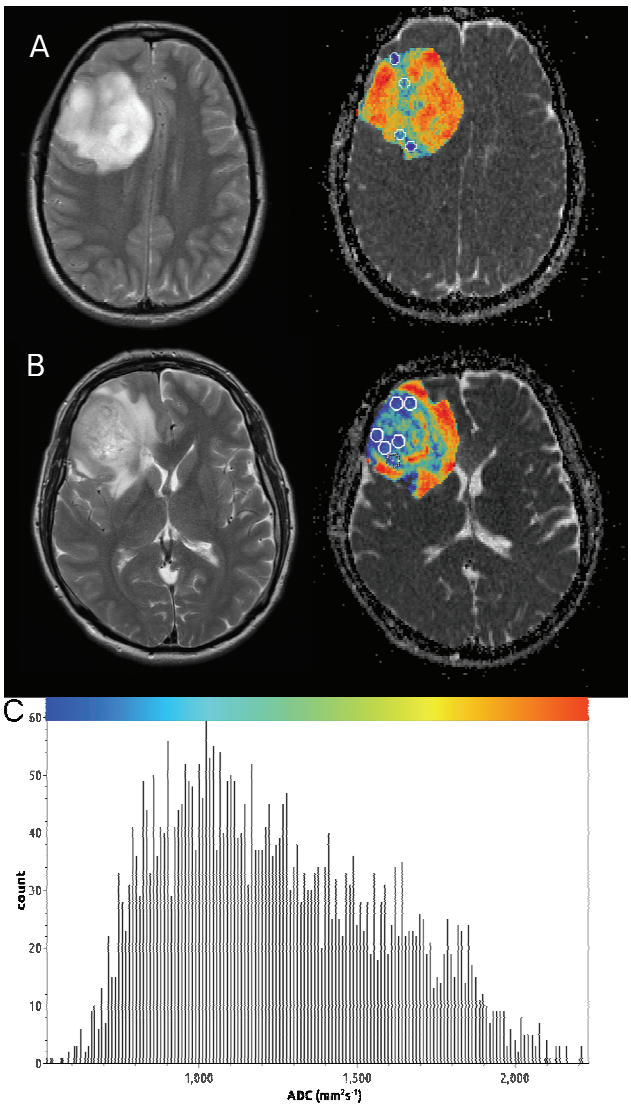

Fig. 1 – The examples of positioning of the regions of interest based on the histogram-based color maps of tumor region in: A) diffuse astrocytoma; B) glioblastoma multiforme; C) The histogram analysis of corresponding color coding of tumor shown in B. ADC – apparent diffusion coefficient.

Statistical analysis

Statistical analysis of the data obtained was performed using the OpenStat software [32]. Normality and homogeneity of the data were tested using the Shapiro-Wilk and Levine's tests. The differences among parameters for astrocytoma groups were assessed using the *t*-test and one-way ANOVA with Bonfferoni correction. The findings were considered significant if $p < 0.05$. The receiver operating characteristic (ROC) curves were generated in order to obtain pairwise comparison between the astrocytoma grades.

Results

The box-whiskers plot in Figure 2 shows the distribution of the ADC values for different astrocytoma grades. The grade II tumors showed the higher ADCs compared with the

grades III and IV, which in turn, had close values (Table I). The significant differences were found between grades II and III ($p < 0.01$) and between grades II and IV ($p < 0.02$), but not between the grades III and IV. A significant difference ($p < 0.001$) was also found when the ADC values of DA were compared to the groups of the HGA (III and IV).

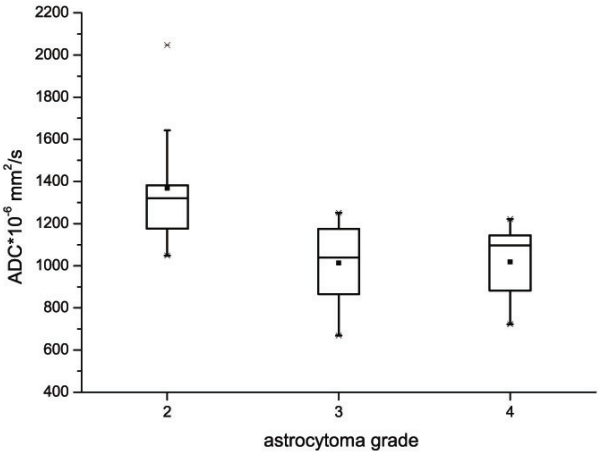

Fig. 2 – Box whiskers plot of the apparent diffusion coefficinet (ADC) values for different astrocytoma grades. The ADC values were measured on the regions of interest placed in regions of the minimal ADC values.

The values of ΔADC, presented by a box-whiskers plot in Figure 3, decreased from grade II to grade III and then rose to grade IV for which the highest values were observed (Table 1). The significant differences were found between the values for the grades II and III, $p < 0.05$), III and IV ($p < 0.001$), but not for II and IV, although there was a trend towards significance. The distribution of kurtosis values for different astrocytoma grades, given in Figure 3, showed the similar trend as for the ΔADC values. The significant differences were found only between the grades III and IV ($p < 0.05$).

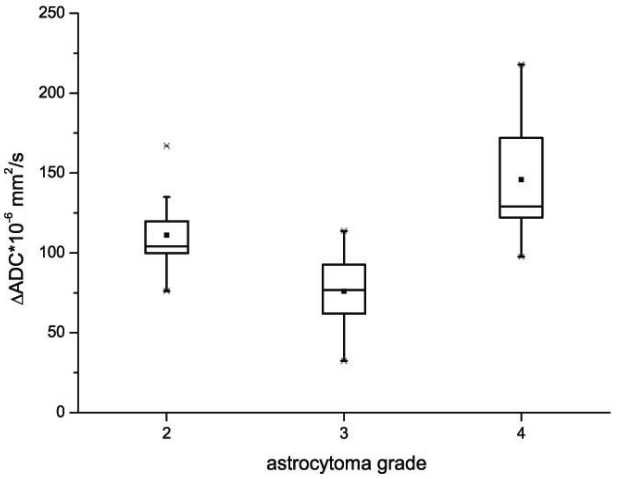

Fig. 3 – Box whiskers plot of standard deviation of the apparent diffusion coefficient (ΔADC) values for different astrocytoma grades measured on the regions of interest placed in regions of the minimal ADC values.

Table 2 shows the results of the ROC analysis of the parameters obtained from the ADC maps in the pairwise comparisons of astrocytic grades. The ΔADC value had the largest area under curve (AUC) among the other analyzed parameters for distinguishing grade 2 from grade 3.

These grades could be distinguished with 78% sensitivity and 89% specificity at the cutoff value of $0.1 \cdot 10^{-3}$ mm^2/s. The ADC value could differentiate between the grades II and III with the same sensitivity, but with somewhat lower specificity (78%) (Figure 4).

Table 1

Average values of ADC, ΔADC and K determined for different astrocytoma grades

Type of astrocytome	ADC·10^{-3} mm^{2}s^{-1}	ΔADC·10^{-3} mm^{2}s^{-1}	K
Astrocytoma grade II	1308 ± 275	111 ± 33	2.8 ± 0.7
Anaplastic astrocytoma (grade III)	1013 ± 217	76 ± 24	2.4 ± 0.4
Glioblastoma multiforme (grade IV)	1019 ± 183	145 ± 41	3.1 ± 0.9

ADC – apparent diffusion coefficient; ΔADC – standard deviation of ADC; K – kurtosis.

Table 2

Results of pairwise ROC analysis for combinations of astrocytoma grades

Parameter	AUC	*p* value	Cutoff	Sensitivity (%)	Specificity (%)
Differentiation between grade 2 *versus* grade 3 astrocytoma					
ADC	0.88	0.01	$1.211 \cdot 10^{-3}$	78	78
ΔADC	0.85	0.007	$0.1 \cdot 10^{-3}$	78	89
K	0.78	0.047	2.76	57	78
Differentiation between grade 3 *versus* grade 4 astrocytoma					
ADC	0.469	> 0.9	$1.100 \cdot 10^{-3}$	67	56
ΔADC	0.975	0.001	$0.17 \cdot 10^{-3}$	100	89
K	0.784	0.042	2.71	78	78

AUC – area under curve; ROC – receiver operating characteristic.
For other abbreviations see under Table 1.

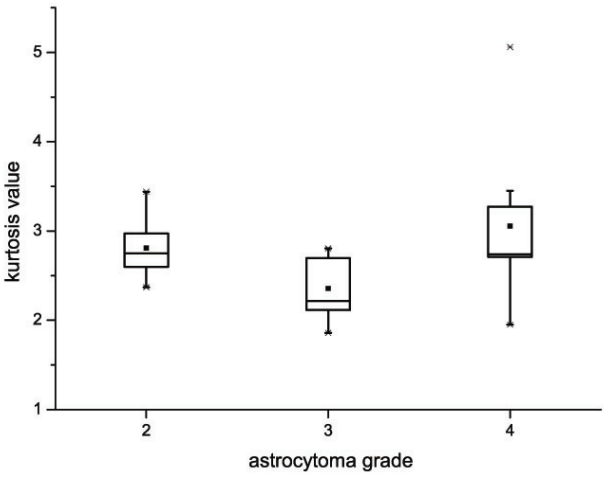

Fig. 4 – Box whiskers plot of the kurtosis values for different astrocytoma grades measured on the regions of interest placed in regions of the minimal apparent diffusion coefficient values.

When distinguishing between the grades III and IV, the ΔADC value had largest AUC (0.975) with sensitivity 100% and specificity 89% and the cutoff value of $0.17 \cdot 10^{-3}$ mm^2/s (Table 2). The kurtosis value could also differentiate between the grades III and IV although with sensitivity and specificity of 78% (AUC = 0.784).

Discussion

Diffusion weighted imaging enables insight into the microstructure of tissues, thus representing an attractive tool for characterization of brain tumors. Here we report the application of DWI in classification of BA. The main accomplishment of the study was the ability to differentiate the gradus III from gradus IV (AA from GBM) using two DWI parameters. The importance of this finding is a potential impact on therapy planning. Treatments are virtually the same for both tumor types – surgery and concomitant radiotherapy and chemotherapy. However, the choice of chemotherapeutic agent for the treatment of primary glioblastoma is narrowed to moderately efficient temozolomide [33], while multiple choices are available for the treatment of AA.

The ADC values of BA obtained in our study are within the range of values reported in a majority of studies [9, 16, 20], but slightly higher than the values obtained by Kitis et al. [17] and Fan et al. [34]. The data analysis showed that ADC values can be used in distinguishing between the astrocytoma grades II and grades III and IV, but not between the last two. This is in agreement with a majority of studies [9, 16–20, 34]. However, there are studies that question the ability of differentiating a low- from a high-grade BA [13–15]. These discrepancies are the most probably the consequence of the procedure of the ROI selection which appears to be extremely important in such highly heterogeneous tumors. For example, in studies where the ROI encompassed the whole tumor no differentiation between the astrocytoma grades was achieved on the basis of mean diffusivity [15, 22]. This can be attributed to masking of cellularity contribution to the average tumor ADC value by contribution of other tumor components such as microcysts, necrosis, bleeding, calcifications, etc. Hence, various other strategies of the ROI selection were employed since the ROIs should reliably represent the most active part of the tumor. In a number of studies, the ROIs were placed on the tumor tissue which appeared as "solid" on the T2W/FLAIR images or enhanced on the T1W images [9, 16, 18, 34, 35]. Some studies used the DWI to select the ROIs [8, 17, 36] under assumption that the minimal ADC values should correlate with the high tumor cellularity and proliferative indexes. The outcome of both approaches was that it was possible to distinguish the low- from high-grade tumors, but not to differentiate the high-grade tumors, i.e., AA from GBM.

The alternative approach, similar to ours, employed the histogram analysis of the whole tumor region in the ADC maps (whole tumor in single ROI) and use only the ADC value of the low edge of the histogram in discriminating grades [22]. This enabled differentiation between the grade II and grade III astrocytoma, but not between the grades III and IV. In our study, we used combined strategy which included an initial histogram analysis of ADC values in whole tumor followed by generation of the histogram-based color maps and placement of ROI in the regions which corresponded to the lowest ADC values. Such approach diminished the influence of subjectivity in the ROI positioning, and more reliable localizations of zones that corresponded to the highest cellularity can be achieved. Nevertheless, we also did not succeed in distinguishing the AA from GBM based on the ADC values.

There are, however, papers where the authors claim that is possible to distinguish the AA from GBM using the ADC data [18, 36, 37]. However, findings of Yang et al. [36] are flawed by the fact that the orientation independent DW image was calculated as an arithmetic mean instead of correct geometric mean. Higano et al. [37] used the method of elimination of the ROIs to the one with a minimal ADC value. The risk of using a single ROI to characterize tumor lies in the fact that such region of the minimal ADC values in the high-grade tumors, besides high cell density, may contain micro bleedings and micro calcifications which could lead to underestimation of the minimal ADCs: these features are more frequent in glioblastomas. Yamasaki et al. [18] used the logistic discriminant analysis to construct classifiers containing both the ADC values of tumors and patient related data (age and gender). This involved the parameters other than those obtained by the MRI and the selection of patients appropriate for inclusion in the analysis.

The lack of difference between the ADCs for the astrocytoma grades III and IV in our study can be explained by similar histopathology of the tumors in the regions that corresponded to high cellularity. Both types are characterized by cell atypia, high mitotic activity and pleomorphism. In addition to this, grade IV is characterized by the presence of ischemic regions and vascular proliferation. However, because of domination of cell component and effects of averaging, these features might not reflect in the ADCs.

Although being the major factor, cell density does not give enough information for histopathological characterization of the brain tumors. Other determinants are cell polymorphism, number of mitoses, density of capillary, presence of micronecrosis and microcalcifications, etc. They have influence on intravoxel and heterogeneity within the ROI, their contribution to tumor ADC values should be considered.

The values of ΔADC obtained in our study enabled differentiation between both the astrocytoma of grades II and III, and also between the grades III and IV. The distribution of the parameter values showed that anaplastic astrocytoma exhibited the lowest heterogeneity in series, followed by the diffuse astrocytoma and glioblastoma multiforme what was in agreement with the microstructure of these tumors [1]. To our knowledge, there are only two studies considering application of this parameter in characterization of the brain pathologies. Bosma et al. [38] found that the ΔADC could be used to discriminate between systemic lupus erythematosus, but surprisingly did not discuss this result. In their study, Kang et al. [22] measured the values of ΔADC of astrocytoma, but did not evaluate the use of this parameter in their differentiation.

The values of kurtosis parameter determined in this study enabled distinguishing the astrocytoma grades III and IV, although with somewhat lower sensitivity and specificity. Kang et al. [22] did not find the significant differences among the kurtosis values of astrocytoma grades which could be explained by the large errors in determination of kurtosis when whole tumor was considered as the ROI. Raab et al. [30] reported ability of excessive kurtosis, obtained from the DTI at the multiple b-values, to differentiate between the astrocytoma grades. However, this procedure (diffusion kurtosis imaging DKI) requires a considerable amount of imaging time and the use of the MRI devices operating at the magnetic fields equal to or higher than 3T [27]. This questions suitability of the DKI in the routine clinical examinations.

Our results suggest that the parameters which characterize heterogeneity of diffusion within defined ROI have advantage over the mean ADC value in differentiation of BA grades III and IV, where the ΔADC value showed the highest sensitivity and specificity. However, it showed similar ability as the mean ADC (although higher specificity) in differentiation grades II and III. The sensitivity and specificity of kurtosis factor in differentiation of these tumor types were somewhat lower compared to that of the ΔADC, but still showed higher performance compared to the mean ADC. This suggests that all determined diffusion parameters should be considered in differentiation of the brain astrocytoma.

The main limitation of this study is a small number of brain astrocytomas included. Analysis of a larger group of tumors may improve the achievements of combination of diffusion parameters in differentiation of the BA. The alternative approach could use the ROI placement based on chemical shift imaging (maps of choline concentrations within lesion) and/or MRI perfusion images, as better indicators of regions of increased cellularity and/or vascularity. We have not included this method in our study, because only two patients had these procedures included in the exam. Further, in this study we did not evaluate diffusion in the peritumoral area or performed normalization to the corresponding values for normal appearing white matter. The reason for such approach was a comparison of successfulness of other parameters derived from the ADC maps measured from the same ROI placed in a lesion; use of normalization would obscure inherent information they contain.

Conclusion

The results presented in this work pinpoint to importance of histogram analysis of the ADC maps in adequate positioning of ROI. Using this approach, it is possible to distinguish the astrocytomas grade II and III using the ADC values. Further analysis of heterogeneity of the ADC values in tumor using the values of ΔADC and kurtosis yielded to even more successful differentiation among astrocytoma grades. Therefore, for overall grading of these tumor types, all three parameters should be used for successful diagnostics.

Acknowledgements

This study was supported by the Ministry of Education, Science and Technological Development of the Republic of Serbia, grant N° III41005.

REFERENCES

1. *Hayat MA.* Tumors of the Central Nervous System: Astrocytomas, Hemangioblastomas, and Gangliogliomas. Volume 5. 1st ed. Dordrecht, Netherlands: Springer; 2011.
2. *Ginsberg LE, Fuller GN, Hashmi M, Leeds NE, Schomer DF.* The significance of lack of MR contrast enhancement of supratentorial brain tumors in adults: Histopathological evaluation of a series. Surg Neurol 1998; 49(4): 436–40.
3. *Roberts HC, Roberts TP, Brasch RC, Dillon WP.* Quantitative measurement of microvascular permeability in human brain tumors achieved using dynamic contrast-enhanced MR imaging: Correlation with histologic grade. AJNR Am J Neuroradiol 2000; 21(5): 891–9.
4. *Lüdemann L, Grieger W, Wurm R, Budzisch M, Hamm B, Zimmer C.* Comparison of dynamic contrast-enhanced MRI with WHO tumor grading for gliomas. Eur Radiol 2001; 11(7): 1231–41.
5. *Le Bihan D.* Molecular diffusion nuclear magnetic resonance imaging. Magn Reson Q 1991; 7(1): 1–30.
6. *Moritani T, Ekholm S, Westesson PL.* Diffusion weighted imaging of the brain. Berlin: Springer-Verlag; 2005.
7. *Johansen-Berg H, Behrens TE.* Diffusion MRI: From quantitative measurement to in-vivo neuroanatomy. San Diego: Academic Press; 2009.
8. *Sugahara T, Korogi Y, Kochi M, Ikushima I, Shigematu Y, Hirai T,* et al. Usefulness of diffusion-weighted MRI with echo-planar technique in the evaluation of cellularity in gliomas. J Magn Reson Imaging 1999; 9(1): 53–60.
9. *Kono K, Inoue Y, Nakayama K, Shakudo M, Morino M, Ohata K,* et al. The role of diffusion-weighted imaging in patients with brain tumors. AJNR Am J Neuroradiol 2001; 22(6): 1081–8.

10. *Calvar JA, Meli FJ, Romero C, Calcagno ML, Yánez P, Martinez AR*, et al. Characterization of brain tumors by MRS, DWI and Ki-67 labeling index. J Neurooncol 2005; 72(3): 273–80.
11. *Chenevert TL, Sundgren PC, Ross BD*. Diffusion imaging: Insight to cell status and cytoarchitecture. Neuroimaging Clin N Am 2006; 16(4): 619–32, viii-ix.
12. *Hayashida Y, Hirai T, Morishita S, Kitajima M, Murakami R, Korogi Y,* et al. Diffusion-weighted imaging of metastatic brain tumors: Comparison with histologic type and tumor cellularity. AJNR Am J Neuroradiol 2006; 27(7): 1419–25.
13. *Lam WW, Poon WS, Metreweli C.* Diffusion MR imaging in glioma: Does it have any role in the pre-operation determination of grading of glioma? Clin Radiol 2002; 57(3): 219–25.
14. *Catalaa I, Henry R, Dillon WP, Graves EE, McKnight TR, Lu Y,* et al. Perfusion, diffusion and spectroscopy values in newly diagnosed cerebral gliomas. NMR Biomed 2006; 19(4): 463–75.
15. *Inoue T, Ogasawara K, Beppu T, Ogawa A, Kabasawa H*. Diffusion tensor imaging for preoperative evaluation of tumor grade in gliomas. Clin Neurol Neurosurg 2005; 107(3): 174–80.
16. *Bulakbasi N, Guvenc I, Onguru O, Erdogan E, Tayfun C, Ucoz T*. The added value of the apparent diffusion coefficient calculation to magnetic resonance imaging in the differentiation and grading of malignant brain tumors. J Comput Assist Tomogr 2004; 28(6): 735–46.
17. *Kitis O, Altay H, Calli C, Yunten N, Akalin T, Yurtseven T*. Minimum apparent diffusion coefficients in the evaluation of brain tumors. Eur J Radiol 2005; 55(3): 393–400.
18. *Yamasaki F, Kurisu K, Satoh K, Arita K, Sugiyama K, Ohtaki M,* et al. Apparent diffusion coefficient of human brain tumors at MR imaging. Radiology 2005; 235(3): 985–91.
19. *Fan G, Zang P, Jing F, Wu Z, Guo Q*. Usefulness of diffusion/perfusion-weighted MRI in rat gliomas: Correlation with histopathology. Acad Radiol 2005; 12(5): 640–51.
20. *Arvinda HR, Kesavadas C, Sarma PS, Thomas B, Radhakrishnan VV, Gupta AK*, et al. Glioma grading: Sensitivity, specificity, positive and negative predictive values of diffusion and perfusion imaging. J Neurooncol 2009; 94(1): 87–96.
21. *Tozer DJ, Jäger RH, Danchaivijitr N, Benton CE, Tofts PS, Rees JH,* et al. Apparent diffusion coefficient histograms may predict low-grade glioma subtype. NMR Biomed 2007; 20(1): 49–57.
22. *Kang Y, Choi SH, Kim Y, Kim KG, Sohn C, Kim J*, et al. Gliomas: Histogram analysis of apparent diffusion coefficient maps with standard- or high-b-value diffusion-weighted MR imaging: correlation with tumor grade. Radiology 2011; 261(3): 882–90.
23. *Beppu T, Inoue T, Shibata Y, Kurose A, Arai H, Ogasawara K*, et al. Measurement of fractional anisotropy using diffusion tensor MRI in supratentorial astrocytic tumors. J Neurooncol 2003; 63(2): 109–16.
24. *Field AS, Alexander AL, Wu Y, Hasan KM, Witwer B, Badie B.* Diffusion tensor eigenvector directional color imaging patterns in the evaluation of cerebral white matter tracts altered by tumor. J Magn Reson Imaging 2004; 20(4): 555–62.
25. *Ferda J, Kastner J, Mukenšnabl P, Choc M, Horemužová J, Ferdová E*, et al. Diffusion tensor magnetic resonance imaging of glial brain tumors. Eur J Radiol 2010; 74(3): 428–36.
26. *Tsuchiya K, Fujikawa A, Nakajima M, Honya K.* Differentiation between solitary brain metastasis and high-grade glioma by diffusion tensor imaging. Br J Radiol 2005; 78(930): 533–7.
27. *Jensen JH, Helpern JA, Ramani A, Lu H, Kaczynski K.* Diffusional kurtosis imaging: The quantification of non-gaussian water diffusion by means of magnetic resonance imaging. Magn Reson Med 2005; 53(6): 1432–40.
28. *Hui ES, Cheung MM, Qi L, Wu EX*. Advanced MR diffusion characterization of neural tissue using directional diffusion kurtosis analysis. Conf Proc IEEE Eng Med Biol Soc 2008; 2008: 3941–4.
29. *Jensen JH, Falangola MF, Hu C, Tabesh A, Rapalino O, Lo C,* et al. Preliminary observations of increased diffusional kurtosis in human brain following recent cerebral infarction. NMR Biomed 2011; 24(5): 452–7.
30. *Raab P, Hattingen E, Franz K, Zanella FE, Lanfermann H*. Cerebral gliomas: Diffusional kurtosis imaging analysis of microstructural differences. Radiology 2010; 254(3): 876–81.
31. *Mcauliffe MJ, Lalonde FM, Mcgarry D, Gandler W, Csaky K, Trus BL*. Medical Image Processing, Analysis and Visualization in clinical research. In: 14th IEEE Symposium on 2001 Computer-Based Medical Systems, CBMS 2001. Proceedings 2011. p. 381–6.
32. *Miller W*. Open Stat Reference Manual. New York, NY: Springer; 2013.
33. *Reardon DA, Wen PY*. Therapeutic advances in the treatment of glioblastoma: Rationale and potential role of targeted agents. Oncologist 2006; 11(2): 152–64.
34. *Fan GG, Deng QL, Wu ZH, Guo QY*. Usefulness of diffusion/perfusion-weighted MRI in patients with non-enhancing supratentorial brain gliomas: A valuable tool to predict tumour grading? Br J Radiol 2006; 79(944): 652–8.
35. *Murakami R, Hirai T, Sugahara T, Fukuoka H, Toya R, Nishimura S,* et al. Grading astrocytic tumors by using apparent diffusion coefficient parameters: Superiority of a one- versus two-parameter pilot method. Radiology 2009; 251(3): 838–45.
36. *Yang D, Korogi Y, Sugahara T, Kitajima M, Shigematsu Y, Liang L,* et al. Cerebral gliomas: Prospective comparison of multivoxel 2D chemical-shift imaging proton MR spectroscopy, echoplanar perfusion and diffusion-weighted MRI. Neuroradiology 2002; 44(8): 656–66.
37. *Higano S, Yun X, Kumabe T, Watanabe M, Mugikura S, Umetsu A,* et al. Malignant astrocytic tumors: Clinical importance of apparent diffusion coefficient in prediction of grade and prognosis. Radiology 2006; 241(3): 839–46.
38. *Bosma GT, Huizinga TW, Mooijaart SP, Van Buchem MA*. Abnormal brain diffusivity in patients with neuropsychiatric systemic lupus erythematosus. AJNR Am J Neuroradiol 2003; 24(5): 850–4.

Received on December 15, 2016.
Accepted on July 06, 2017.
Online First September, 2017.